



Low-dimensional systems on the base of PbSnAgTe (LATT) compounds for thermoelectric application

Lyubomyr Nykyruy^{a,*}, Mark Ruvinskiy^a, Eugeny Ivakin^b, Oksana Kostyuk^a, Ihor Horichok^a, Ivan Kisialiou^b, Yaroslav Yavorsky^a, Andriy Hrubyak^a

^a Vasyl Stefanyk Precarpathian National University, Ivano-Frankivsk, Ukraine

^b B.I. Stepanov Institute of Physics NAS of Belarus, Minsk, Belarus

ARTICLE INFO

Keywords:

Thermoelectric properties
Quantum-size effects
Nanoscale thin films
LATT
Carrier scattering

ABSTRACT

In the paper the p-type of conductivity polycrystalline thin films were received on the basis of PbSnAgTe (LATT) materials deposited on the mica-muscovite substrate. The temperature and thickness dependences of conductivity, current carriers mobility and specific thermoelectric power were investigated for these films. It is shown that scattering on acoustic phonons is the dominant mechanism at above room temperature. The presence of oscillations in profiles of thermoelectric parameters of specific electrical conductivity and Seebeck coefficients is experimentally obtained. The theoretical explanation of oscillations is explained within the framework of model of rectangular potential well with infinitely high walls. The estimation of the efficiency of thermoelectric materials, namely, the dimensionless thermoelectric figure of merit is $ZT \sim (1.2-1.5)$.

1. Introduction

The engineering of materials for efficient and inexpensive renewable energy sources is the highest priority area of modern applied research. The importance is due to the awareness of the exhaustion of fossil fuels and significant emissions of greenhouse gases into the atmosphere after burn off that pollute the environment, damage the ozone layer of the Earth, and cause global climate change. The studies on the direct conversion of thermal energy into electricity are very important. One of the main arguments is that thermoelectric energy transformers are among the most reliable sources of electricity allowing continuous operation for decades [1–3]. The efficiency of thermoelectric materials is determined by the dimensionless thermoelectric figure of merit (ZT) (otherwise: thermoelectric quality factor):

$$zT = S^2\sigma T / (\kappa_E + \kappa_L),$$

where S , σ , T , κ_E , and κ_L represent the Seebeck coefficient, electrical conductivity, absolute temperature, and electronic and lattice contributions to the total thermal conductivity κ , respectively [1].

The most interesting and valuable materials are those that work most efficiently in the temperature range (450–800) K. The greatest amount of heat into environment is generated from industrial objects just in this temperature range [4]. Therefore, the possibility of re-use of

this heat to generate thermoelectric energy has an economic and environmental value. The compounds based on IV-VI semiconductors are the most known and promising materials for such use [5–9]. Moreover, new materials known as LAST (Lead-Antimony-Silver-Telluride: Pb-Ag-Sb-Te) were obtained by doping of the main matrix which were characterized by high values of $ZT > 1$ at temperatures $T > 600$ K [10–13]. Also, the thermoelectric properties of LAST compounds essentially depend on the chemical composition [12–18]. It is also possible to change the type of conductivity of the material by controlling the chemical composition, which makes the system particularly promising for use in power generation [19–21].

A lot of theoretical and experimental studies have shown that the use of low-dimensional systems greatly improves the thermoelectric properties [22–24].

One of the technologically simple solutions is to obtain 2D-systems, in particular, thin films [25–28]. Study of the dimensional effects in thin films makes it possible to obtain the high values of the thermoelectric figure of merit (ZT) [1,29,30]. The manifestations of the quantum-size effects that occur in non-doping PbTe films are of the particular interest [31]. The anisotropy of effective masses is observed for the materials on the base of IV-VI compounds and effective mass is sufficiently small in the one of directions (it is $m_z = 0.022 m_e$ for p-PbTe) [31–38]. Therefore, it is possible to improve the thermoelectric

Abbreviations: LAST, Lead Antimony Silver Telluride; LATT, Lead Argentum Tin Telluride; AFM, Atomic force microscopy

* Corresponding author.

E-mail address: lyubomyr.nykyruy@gmail.com (L. Nykyruy).

<https://doi.org/10.1016/j.physe.2018.10.020>

Received 18 March 2018; Received in revised form 2 October 2018; Accepted 12 October 2018

Available online 15 October 2018

1386-9477/ © 2018 Elsevier B.V. All rights reserved.

figure of merit due to oscillations in the profiles of specific conductivity and the Seebeck coefficient.

The potential features of the LATT type of semiconductors (Lead-Argentum-Tin-Telluride) [39] should be highlighted among the new multicomponent materials. The possibility of smooth control of technological parameters predicts the possibility of obtaining cheap material with the high ZT values.

In this paper analysis of the p-type of conductivity thin films of the LATT system, obtained by open evaporation in vacuum on the fresh chips (0001) of mica-muscovite substrates, was performed. The peculiarities of changes of thermoelectric parameters of these films on temperature and chemical composition have been investigated. Particular attention is focused on the analysis of the quantum-size effects in obtained nanoscale films to improve their thermoelectric efficiency.

2. Experiment

Synthesis of PbSnAgTe materials was carried out in the vacuum quartz ampoules pressurized to residual pressure 10^{-4} Pa. The ampoules were pre-cleaned, namely, by washing in a mixture of $\text{HNO}_3\text{:HCl:H}_2\text{O}$ for 3 h with next multiple washing by distilled water and alcohol, and drying in an oven at $T = (450\text{--}500)$ K [12].

For synthesis high-purity initial components were used: purified Lead with 99.99% of the main component, and Silver, Tin and Tellurium with purified of 99.999%. The vacuum ampoules with initial components were placed in a muffle furnace horizontally. To avoid a sharp increase of the tellurium steam pressure in the ampoule and to create conditions for the best mixing of molten components, the synthesis was carried out in several stages: heating up to 500 °C (the temperature change velocity was 17 °C/min), next 1 h of exposure; heating up to 700 °C (7 °C/min), 3 h of exposure; heating up to 1020 °C (11 °C/min), 1 h of exposure; cooling to 900 °C (4 °C/min); quenching in the air.

The phase composition and structure of the synthesized ingots were investigated by X-diffraction methods on the STOE STADI P automatic diffractometer (manufactured by STOE & Cie GmbH, Germany) with a linear position-precision detector PSD according to the modified Giniere geometry scheme. Calculation of theoretical diffraction patterns for known compounds for phase identification and definition of unit cell parameters was performed with software packages STOE WinXPOW (version 3.03) and PowderCell (version 2.4). Refinement of crystalline structure phases for studied samples in the isotropic approximation for atomic displacement parameters was carried out by the Rietveld method using PseudoVoigt profile function with the help of FullProf.2k (version 5.30) from the WinPLOTR software package. Perhaps the predominant orientation (texture) of main phase grains was determined by function of the Marsh-Dallas prevailing orientation. Quantitative phase analysis was performed by refining the Rietveld method using Hill and Howard's technique [40].

The studied samples were obtained by depositing of the vapor of synthesized PbTe [41], $\text{Pb}_{1.4}\text{Sn}_4\text{Ag}_2\text{Te}_{20}$, $\text{Pb}_{1.6}\text{Sn}_2\text{Ag}_2\text{Te}_{20}$ and $\text{Pb}_{1.8}\text{Ag}_2\text{Te}_{20}$ materials in vacuum under fresh chips (0001) mica-muscovite substrates. The temperature of the evaporator was $T_E = 870$ K, and the temperature of the substrates was $T_p = 470$ K. The thickness of the films was determined by deposition time within (1–3) min and measured using a micro-interferometer MII-4 and Dektak XT profilograph with digital image processing methods.

The Hall measurements of electrical parameters of the thin films were carried out at the temperature $T = (290\text{--}390)$ K in constant magnetic field at the automated device DHM-1 [42]. The measured sample had four Hall's and two current contacts. The silver was deposited for forming Ohmic contact. The current through the samples was ≈ 1 mA. The magnetic field with induction $B = 1.2$ T directed perpendicular to the film plane.

The X-ray fluorescence spectrum was obtained using the Expert-3L

spectrometer (channel width (118 ± 7) eV).

An integral method was used to measure the Seebeck coefficient S . In this case the one edge of the film had constant temperature, and the temperature of the other edge was changed. The edges of the film are attached to massive copper plates to provide a constant temperature. The temperature was measured using platinum thermistors. Measurement error is no more than 5%. The type of charge carriers is determined by the sign of the Hall constant R_H and of the Seebeck coefficient S .

Heat transfer properties of films as being the parameter of importance in thermoelectric devices were studied by contactless optical method of transient grating, using laser-based system "Optopicotest" developed in the Institute of Physics, National academy of sciences of Belarus [43]. Accordingly to the approach, free surface of film is irradiated by two interfering beams at 533 nm wavelength from pulsed laser. Thermal dilation of subsurface layer of film caused by laser radiation absorption appeared to be spatially modulated so that a relief transient grating is recorded. The grating of thermorefectance is also formed on the film surface. However, its yield to the diffracted signal is experimentally estimated to be small in comparison with that of the relief grating. Heat transfer vector lies in film surface and is directed parallel to the grating vector.

The transient gratings is readout by beam from He-Ne CW laser in reflection mode and intensity of diffracted signal is detected with proper temporal resolution. Lifetime and spacing of thermal grating are the parameters to be measured experimentally. The in-plane thermal diffusivity of films is calculated by using theoretical model worked out, taking into account the results of Johnson [44].

3. Results and discussion

The diffraction patterns of the $\text{Pb}_{1.6}\text{Sn}_2\text{Ag}_2\text{Te}_{20}$ and $\text{Pb}_{1.4}\text{Sn}_4\text{Ag}_2\text{Te}_{20}$ solid solutions are shown in Fig. 1. The main phase is PbTe, the structural type is NaCl, and the additional phase is $\text{Ag}_{10.6}\text{Te}_7$. For the samples with less content of the tin, the elementary cell parameter is 6.4402(2) Å, and with a larger one is 6.4413(3) Å.

The chemical analysis of the PbTe film was carried out using X-ray fluorescence spectra. The identification of the chemical elements was carried out according to the energies in which the main peaks on the spectrum were observed and compared with the tabular data. In this case, there were no additional chemical elements in the investigated film (Fig. 2). The background peaks correspond to the chemical composition of the mica-muscovite substrate. The mass ratio Pb: Te for PbTe film on the mica-muscovite substrate is 65: 35 within the relative error $\pm 3\%$ (Table 1). Also, there is a small amount of oxygen $\sim 0.5\%$ in the film. We can summarize that the processes of adsorption of the oxygen by surface and its penetration into the depth of the film for these compositions are negligible.

The AFM-images of the films surface of the research samples are shown in Fig. 3. All the samples have a polycrystalline structure. The features of the carriers transport mechanisms in polycrystalline films are determined both by the volume of grain and inter-granular barriers [45]. However, as it was reported before [39,45], for the films of the studied compositions the effect of the boundaries is significant for low temperatures $T < 170$ K. Therefore, for the studied temperature range $T = (290\text{--}390)$ K, the effects associated with scattering on the grain boundary were not considered.

The Hall's mobility is the main parameter that characterizes the mechanisms of electron transport. It rapidly decreases with temperature (Fig. 4). The temperature dependence of the carrier mobility in the coordinates $\ln \mu$ due $\ln T$ will be linear (Fig. 4b). We see that the coefficient of inclination is very close to $-5/2$ for all studied compositions. Such value of the angular coefficient is most generally found for PbTe compounds at high carrier concentrations and temperatures above 300 K [25,31,36]. For the nondegenerate statistics of carriers, the carrier mobility (in this case, the holes) due to scattering on long-wave

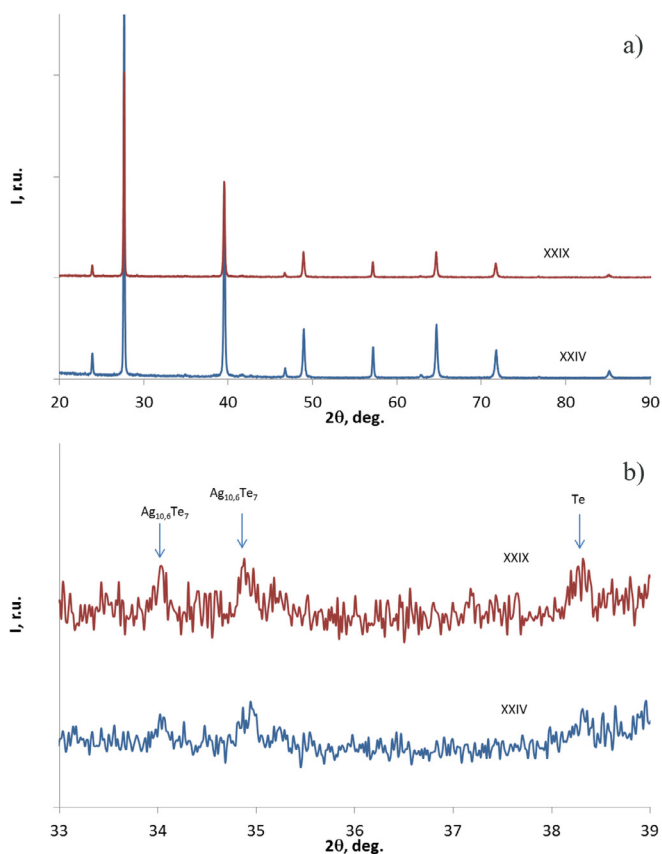


Fig. 1. The diffraction patterns of the $Pb_{16}Sn_2Ag_2Te_{20}$ (XXIV) and $Pb_{14}Sn_4Ag_2Te_{20}$ (XXIX) solid solutions (a) and the fragment of the diffractogram in the region of the detected of reflexes of the additional phases (b).

acoustic oscillations was determined by the formula

$$\mu_a \sim m^{-5/2} T^{-3/2}. \tag{1}$$

It should be noted that the effective mass of PbTe also increases with increasing of the temperature according to the law of $m^{0.4}$ for holes for the investigated temperature range (300–400) K [36]. This is explained by the fact that with increasing of the temperature the number of carriers with high energy increases, which is characterized by large effective mass. Taking into account the temperature dependence of the effective mass we can obtain the index of degree $-5/2$. Moreover, the main mechanism of carrier scattering is the scattering on acoustic phonons.

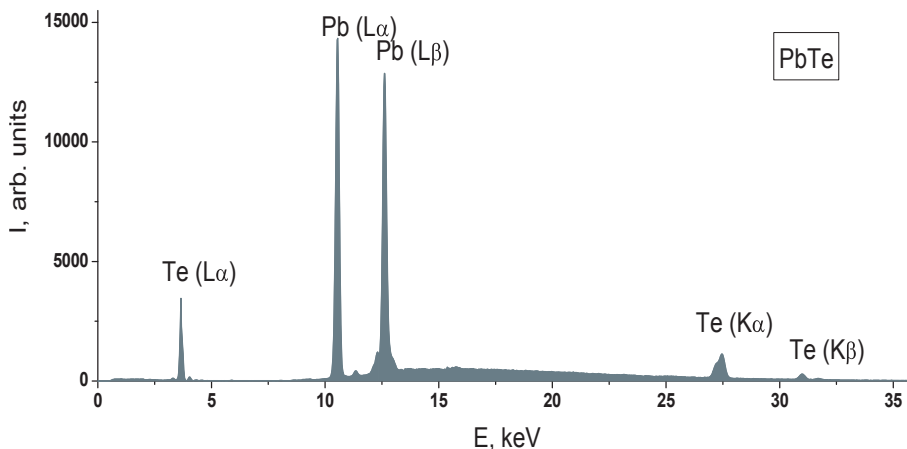


Fig. 2. X-ray fluorescence spectrum of PbTe film on mica-muscovite substrate.

Table 1
The mass ratio of chemical elements for PbTe films on the mica-muscovite substrate.

Chemical element	Mass ratio, %
^{16}O	0.578 ± 0.115
^{52}Te	35.066 ± 2.274
^{82}Pb	64.324 ± 2.972
Calculation data for chemical formulas	
Chemical formula	Mass ratio, %
PbO	7.954
PbTe	92.007

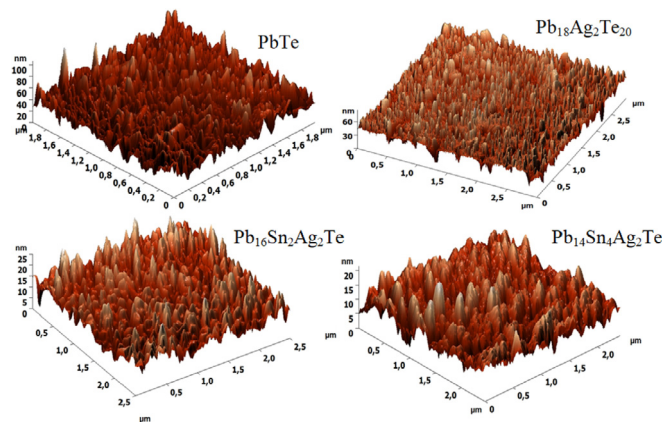


Fig. 3. AFM-images of the surface of $Pb_{m-x}Sn_xAg_2Te_m$ films on mica-muscovite substrates (thickness of all films $d = 1.08 \mu m$, temperature of substrate $T_s = 500 K$).

Temperature dependences of the specific electrical conductivity (σ), of the concentration of current carriers (p), of the Seebeck coefficient (S), and of the thermoelectric power ($S^2\sigma$) for the films based on PbSnAgTe compounds deposited on the mica-muscovite substrates are shown in Figs. 5–7, respectively.

For non-doping PbTe and $Pb_{18}Ag_2Te_{20}$ films an activation mechanism of conductivity is observed. That is, the conductivity increases with increasing of the temperature according to the formula [31]

$$\sigma = \sigma_0 \exp\left(-\frac{E_a}{k_B T}\right) \tag{2}$$

The activation energies were determined from the experimental data. They are 59.8 meV and 60.4 meV for PbTe and $Pb_{18}Ag_2Te_{20}$,

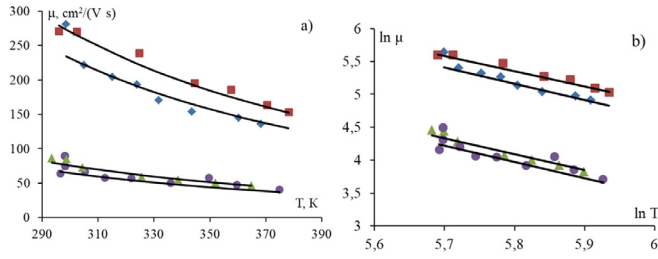


Fig. 4. Temperature dependence of Hall mobility (μ) (a), and logarithm dependence of mobility ($\ln \mu$) due ($\ln T$) (b) for the films of the next compositions: \blacktriangle - PbTe, \blacksquare - $\text{Pb}_{14}\text{Sn}_4\text{Ag}_2\text{Te}_{20}$, \blacklozenge - $\text{Pb}_{16}\text{Sn}_2\text{Ag}_2\text{Te}_{20}$, \bullet - $\text{Pb}_{18}\text{Ag}_2\text{Te}_{20}$ on fresh (0001) mica-muscovite substrate. Points are the experiment, and lines – approximation by formula (1).

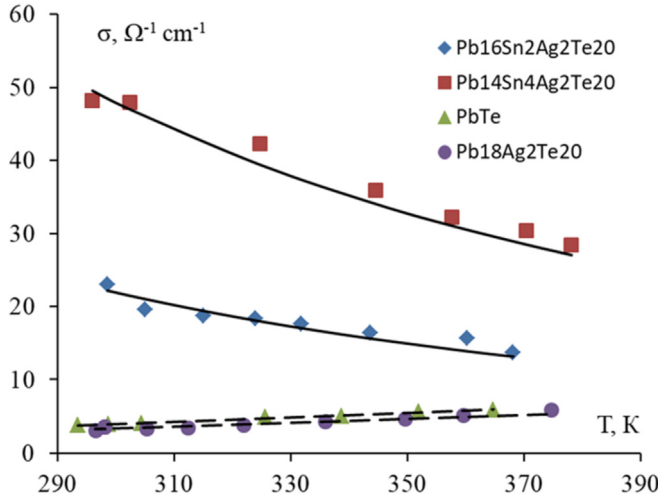


Fig. 5. Temperature dependence of the specific electrical conductivity (σ) for the films of the next compositions: \blacktriangle - PbTe, \blacksquare - $\text{Pb}_{14}\text{Sn}_4\text{Ag}_2\text{Te}_{20}$, \blacklozenge - $\text{Pb}_{16}\text{Sn}_2\text{Ag}_2\text{Te}_{20}$, \bullet - $\text{Pb}_{18}\text{Ag}_2\text{Te}_{20}$ on fresh (0001) mica-muscovite substrates. Solid lines – calculation by formula (3), dashed lines – approximation by formula (2).

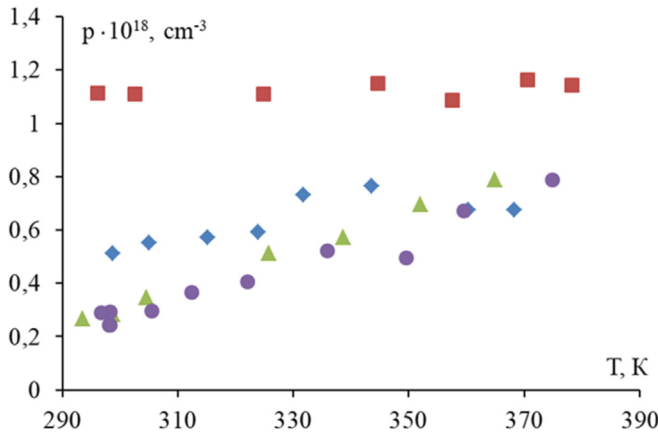


Fig. 6. Temperature dependence of Hall concentration (p) for the films of the next compositions: \blacktriangle - PbTe, \blacksquare - $\text{Pb}_{14}\text{Sn}_4\text{Ag}_2\text{Te}_{20}$, \blacklozenge - $\text{Pb}_{16}\text{Sn}_2\text{Ag}_2\text{Te}_{20}$, \bullet - $\text{Pb}_{18}\text{Ag}_2\text{Te}_{20}$ on fresh (0001) mica-muscovite substrates.

respectively. It can be seen that for $\text{Pb}_{14}\text{Sn}_4\text{Ag}_2\text{Te}_{20}$ and $\text{Pb}_{16}\text{Sn}_2\text{Ag}_2\text{Te}_{20}$ films the conductivity decreases with increasing of the temperature. Such decreasing of conductivity with increasing of the temperature is explained by the decrease carrier mobility, since the concentration for these samples (Fig. 6) weakly depends on the temperature in this temperature range [31]:

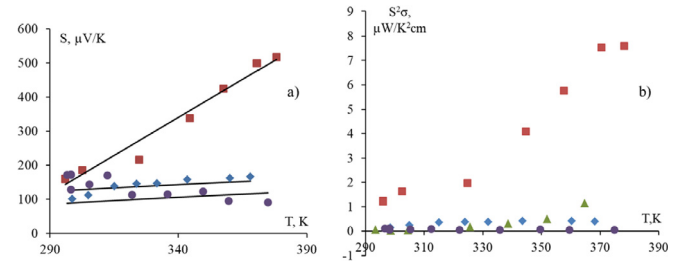


Fig. 7. Temperature dependence of specific thermoelectric power ($S^2\sigma$) for the films of following compositions: \blacktriangle - PbTe, \blacksquare - $\text{Pb}_{14}\text{Sn}_4\text{Ag}_2\text{Te}_{20}$, \blacklozenge - $\text{Pb}_{16}\text{Sn}_2\text{Ag}_2\text{Te}_{20}$, \bullet - $\text{Pb}_{18}\text{Ag}_2\text{Te}_{20}$ on fresh (0001) mica-muscovite substrate.

$$\sigma = e p \mu; \quad (3)$$

The temperature dependence of the Hall carrier concentration (p) is shown in Fig. 6. All investigated samples have the p-type of conductivity. This is confirmed by measurements of the Seebeck coefficient (S) (Fig. 7a). The admixture of silver in the PbTe exhibits amphoteric properties, and it reduces the thermal conductivity [17,25]. But there are no significant changes for electrical parameters. We obtained the p-type of conductivity after addition of the Tin atoms. Moreover, the carrier concentration increases with increasing of the content of Tin (Fig. 6).

The increasing of the Seebeck coefficient (S) and the thermoelectric power ($S^2\sigma$) with increasing of the temperature (Fig. 7) is observed for all compositions of the studied films. Moreover, it is the largest for $\text{Pb}_{14}\text{Sn}_4\text{Ag}_2\text{Te}_{20}$ films due to the high values of their Seebeck coefficient and conductivity values.

The behavior of the dependence curves of the Seebeck coefficient and the concentration for some sample compositions are different. Therefore, the description of the $S(T)$ dependences is carried out, assuming that the charge carrier statistics of the film can be degenerate or non-degenerate.

For a non-degenerate case the Seebeck coefficient (S) is defined as

$$S = \frac{3}{2} \frac{k_B}{e} + const, \quad \frac{3}{2} \frac{k_B}{e} = 129 \text{ mK/B/K} \quad (4)$$

We suggested in (4) that the concentration, effective mass, and the dispersion parameter (r) are not temperature dependent.

For the degenerate statistics of charge carriers, the Seebeck coefficient increases proportionally with the increase of temperature

$$S = \frac{2\pi^{2/3} k_B^2 m^* (r + 3/2)}{3^{5/3} e \hbar^2 p^{2/3}} \cdot T + const. \quad (5)$$

As it is shown in Fig. 4 the carrier statistics are nondegenerate for $\text{Pb}_{16}\text{Sn}_2\text{Ag}_2\text{Te}_{20}$ and $\text{Pb}_{18}\text{Ag}_2\text{Te}_{20}$ films, and the coefficient before $\ln(T)$ is very close to the theoretically predicted value. A slight deviation can be due to the temperature dependence of concentration, effective mass, and dispersion parameter. For the $\text{Pb}_{14}\text{Sn}_4\text{Ag}_2\text{Te}_{20}$ film the electron gas of the current carriers is degenerate, and the Seebeck coefficient increases proportionally with the increase of temperature (T). Also, the carriers concentration for this composition is the highest and it is $1.1 \cdot 10^{18} \text{cm}^{-3}$. Such behavior of the carriers in $\text{Pb}_{14}\text{Sn}_4\text{Ag}_2\text{Te}_{20}$ films allows them to be used to realize the quantum-size effects.

The thermal conductivity was the smallest for the bulk samples $\text{Pb}_{14}\text{Sn}_4\text{Ag}_2\text{Te}_{20}$ and equaled $\kappa = 3 \cdot 10^{-3} \text{ W/(cm}\cdot\text{K)}$ [26]. Thus, it is possible to estimate the value of the thermoelectric figure of merit (ZT). This makes it possible to assume that the films based on this chemical composition will be characterized by high thermoelectric efficiency $ZT = 1$ at temperature of 380 K (see Fig. 8). Consequently, the films on the base of $\text{Pb}_{14}\text{Sn}_4\text{Ag}_2\text{Te}_{20}$ can be used as p-branches for the high-efficiency thermoelectric energy converters.

Also the coefficient of the thermal conductivity can be defined from investigation of the behavior of thermal diffusivity.

Films whose thickness is larger than $1 \mu\text{m}$ were selected for the in-

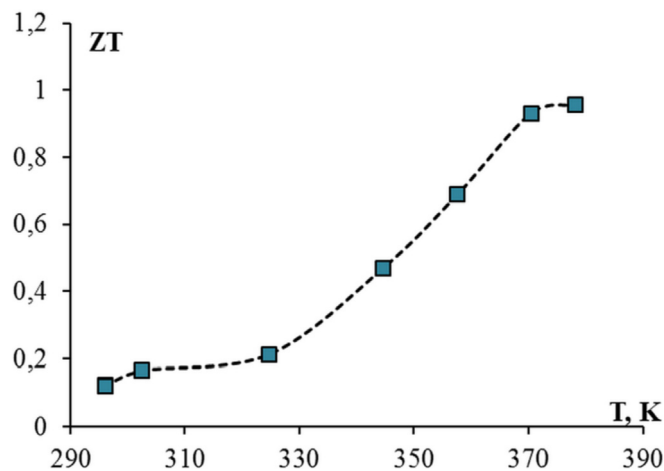


Fig. 8. Temperature dependence of the thermoelectric figure of merit (ZT) for $Pb_{14}Sn_4Ag_2Te_{20}$ films deposited on fresh (0001) mica-muscovite substrate.

plane thermal diffusivity measurement. This is because theoretical estimations show that with grating spacing $5\ \mu m$ used in experiment, the results of measurement provide effective thermal diffusivity of system film/substrate rather than that of film itself if film thickness is less than $1\ \mu m$.

Thermal excitation of films was carried out by laser pulses of 8 ns duration and energy density of about $3\ mJ/cm^2$. Diameter of the excitation beam on the sample plane was 1.5 mm. Accordingly to calculation with film absorption coefficient of order $5 \cdot 10^4\ cm^{-1}$ an average temperature in the excitation spot at the moment of laser beam action rose about $60\ ^\circ C$ above room temperature. The height of the surface relief as determined from the diffraction efficiency of thermal grating was several \AA .

Typical oscillogram of diffracted signal decay is shown in Fig. 9. It worth to note that thermal diffusivity of non-doped bulk single crystalline PbTe is $1.8 \cdot 10^{-2}\ cm^2/s$ [46] whereas the same material in form of $5\ \mu m$ thick film grown on BaF_2 substrate gives $1.3 \cdot 10^{-2}\ cm^2/s$ [43]. Authors see this reduction is because of high dislocation density in film due to the lattice parameter mismatch. Similar tendency of the thermal diffusivity lowering one can notice in Table 2.

The estimate of the thermal conductivity can be carried out in accounting of model of the Debye's phonons spectrum:

$$\kappa = \alpha C_p D.$$

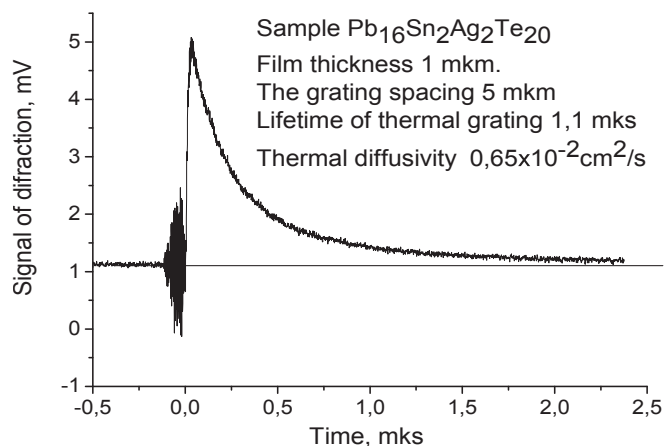


Fig. 9. Kinetics of the diffraction signal for the $Pb_{16}Sn_2Ag_2Te_{20}$ film. After the recording noise, the rapidly increasing part of the kinetics is determined by the time of the exciting pulse duration. The decaying component of the signal is used for thermal diffusivity calculation. The main results of the measurements conducted are summarized in Table 2.

Table 2

Thermal diffusivity for investigated LATT films on mica-muscovite substrate.

Type of the film	Thermal diffusivity, $10^{-2}\ cm^2/s$
Non-doped PbTe	1.4–1.5
$Pb_{18}Ag_2Te_{20}$	1.0–0.9
$Pb_{14}Sn_4Ag_2Te_{20}$	0.8–0.9
$Pb_{16}Sn_2Ag_2Te_{20}$	0.6–0.8

In this equation α is the thermal diffusivity, D is density of the material, C_p is heat capacity.

On the basis of our data for the studied materials it is easy to obtain, $\kappa \sim 0.002449\ W/(cm \cdot K)$ at 300 K. Therefore, in this case the estimated thermoelectric figure of merit is $ZT \sim 0.5$ for 300 K and $ZT \sim 1.17$ at 400 K.

However, a series of publications indicates the possibility of quantum-size effects realization in thin semiconductor films [22–25]. The authors of these publications showed significantly improved thermoelectric parameters.

The quantum-size effects cause the oscillations of thermoelectric parameters.

The ostent of the quantum-size effects can be observed experimentally from the AFM-analysis. The AFM-images of the film surface is presented in Fig. 10. We see that the surface of the observed films is smooth, although it is possible to observe some pyramidal heterogeneities (Fig. 10). As shown on profilograms of surface, the average height of these inhomogeneities is $H = 1.7\ nm$ (Fig. 10b). It should also be noted that the average roughness of the film surface is $S_a \approx 0.35\ nm$ (thickness of the film is $d = 100\ nm$). This satisfies one of the terms for the ostent of the quantum-size effect that the film should be sufficiently homogeneous in thickness. Thus, the $Pb_{14}Sn_4Ag_2Te_{20}$ film has a high homogeneity and a smooth surface. There are also no defects of macroscopic size (pores, cracks, etc.) (Fig. 11).

The coefficient of mirroring of carriers dispersion on surface can be estimated from the Zaiman model, knowing the surface roughness by the formula [17]:

$$p = \exp\left(-\frac{16\pi^3 Z^2}{l^2}\right). \tag{6}$$

The calculated value of the coefficient of mirroring is $p = 0.99$ at the run length $\lambda = 100\ nm$, which is very close to "1". Therefore, we can assume that the carriers scattering in thin films based on $Pb_{14}Sn_4Ag_2Te_{20}$ is fully mirroring.

For the dimensional quantization, it is also necessary that the size of the crystallites exceeds the thickness of the films (d), in order to avoid the effect of scattering on the grain boundaries. For example, the AFM data shown that the experimental value of the grain size was $D = 430\ nm$ at the thickness $d = 100\ nm$, which is four times more than the thickness of the film.

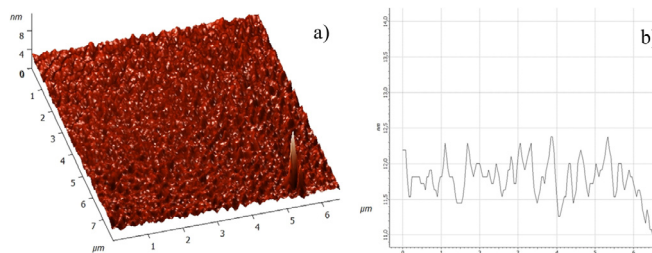


Fig. 10. 3D- AFM-image (a) and profilogram of surface (b) of the $Pb_{14}Sn_4Ag_2Te_{20}$ thin films deposited of (0001) mica-muscovite substrate (thickness $d = 100\ nm$).

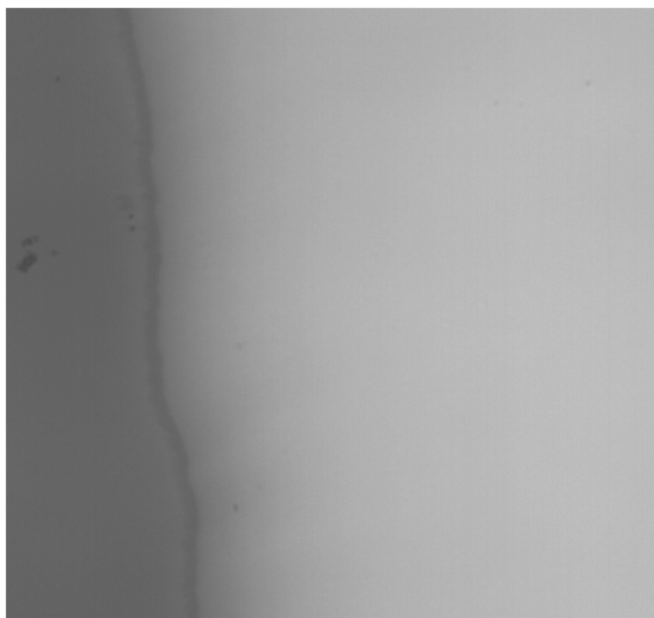


Fig. 11. Microphotography of the boundary of substrate section (film measuring is 120×120 microns).

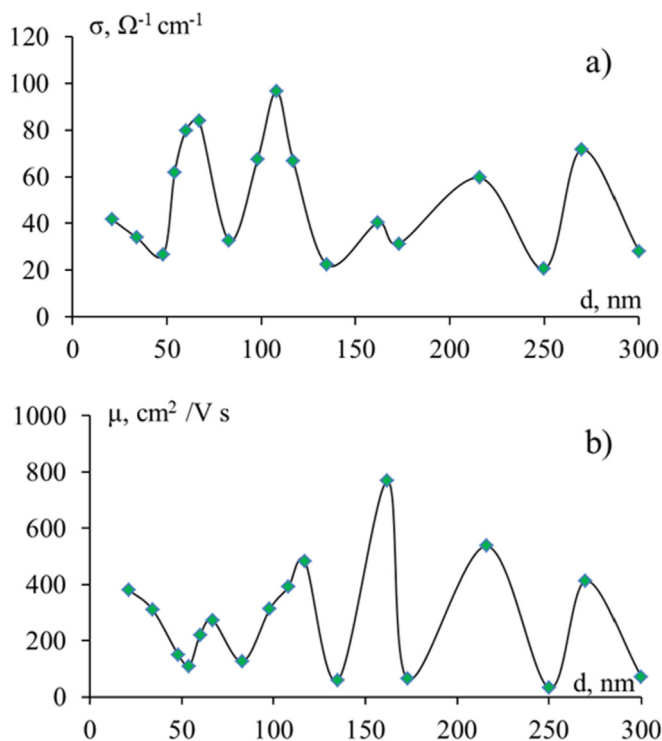


Fig. 12. The thickness dependence of the specific conductivity (σ) (a) and Hall mobility (μ) (b) for $\text{Pb}_{14}\text{Sn}_4\text{Ag}_2\text{Te}_{20}$ films deposited on (0001) mica-muscovite substrate in the case of degenerate electron gas. Points are the experiment.

It is necessary to check the possibility of realizing the quantum-size effect in these films [23]. For $\text{Pb}_{14}\text{Sn}_4\text{Ag}_2\text{Te}_{20}$ films ($m^*_{\perp} = 0.021 m_0$ and $m^*_{\parallel} = 0.31 m_0$) [33] with thickness $d = 10$ nm, the distance between adjacent sub-bands define as $\Delta E = \varepsilon_1 (2n + 1)$. We received $\Delta E \approx 538$ meV for $n = 1$, and the thermal blurring of sub-bands at room temperature is $k_B T = 25.8$ meV. Thereby, the condition that at least several sub-bands are located under the Fermi level was executed. The high carrier's mobility in thin films is satisfied with the condition of long path length (Fig. 12). The de Broglie wavelength ($\lambda_D = 2\Delta d$)

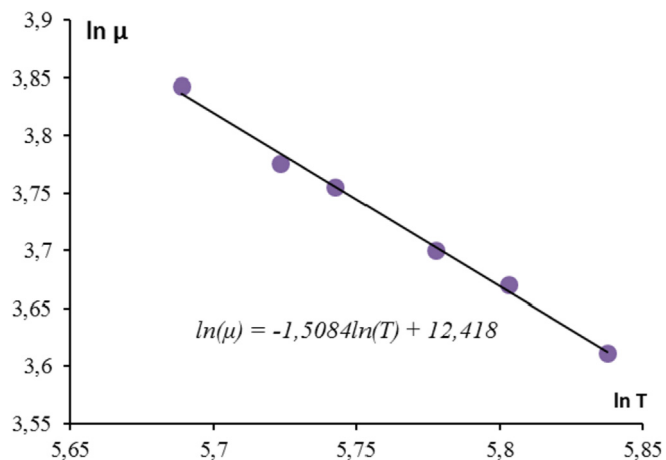


Fig. 13. The dependence of logarithm of mobility ($\ln \mu$) due the logarithm of temperature ($\ln T$) for $\text{Pb}_{14}\text{Sn}_4\text{Ag}_2\text{Te}_{20}$ films.

exceeds the roughness of the films ($S_a \approx 0.35$ nm).

One of the assumptions of the theory of quantum-size effect is the electron energy independent relaxation time [33]. Therefore, the carrier scattering on acoustic phonons in two-dimensional film is considered. To verify this assertion, the measurements of the temperature dependence of the Hall mobility of current carriers in thin film (with thickness $d = 80$ nm) were carried out. Consider the dependence of $\ln(\mu) = f(\ln T)$ to determine the carrier scattering mechanism (Fig. 13). The figure shows that the angular coefficient is -1.5 . Therefore, the dominant carrier scattering mechanism is the scattering of carriers on long-wave acoustic oscillations [25]. And for scattering on acoustic phonons, the relaxation time does not depend on the energy ($\tau = \tau_0$).

All of the above terms confirm the possibility of interpreting the observed oscillations of thermoelectric parameters within the framework of the quantum-size effect theory.

In Figs. 12 and 13 the dependences of the specific electrical conductivity (σ), Hall mobility (μ), and the Seebeck coefficient (S) are shown for the thin films of $\text{Pb}_{14}\text{Sn}_4\text{Ag}_2\text{Te}_{20}$ at room temperature $T = 300$ K. As we can see from experimental data the oscillations are observed in the profiles of the thermoelectric parameters $\sigma(d)$, $\mu(d)$, S (d) and $S^2\sigma(d)$ in the thickness range $d = (20\text{--}270)$ nm. Figs. 12, 14 and 15 show that the period of oscillations is (40–50) nm.

It is worth noting that the maxima and minima on the $\sigma(d)$ and $\mu(d)$ dependences coincide. Accordingly, the maxima and minima of the

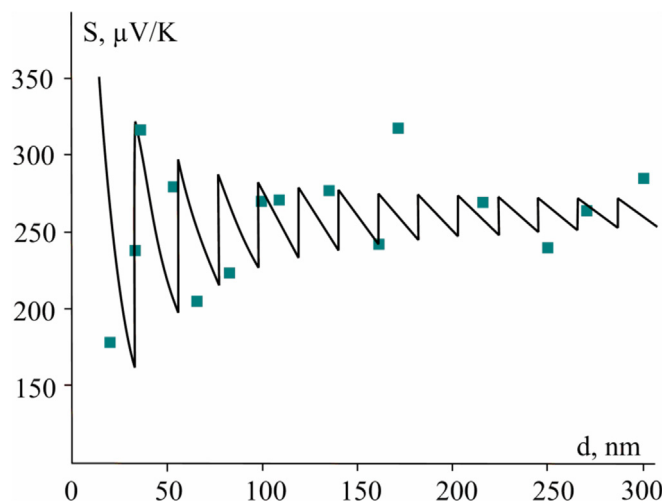


Fig. 14. The thickness dependence of the Seebeck coefficient (S) for $\text{Pb}_{14}\text{Sn}_4\text{Ag}_2\text{Te}_{20}$ films deposited on (0001) mica-muscovite substrates in the case of degenerate electron gas. Points are the experiment, line is a calculation.

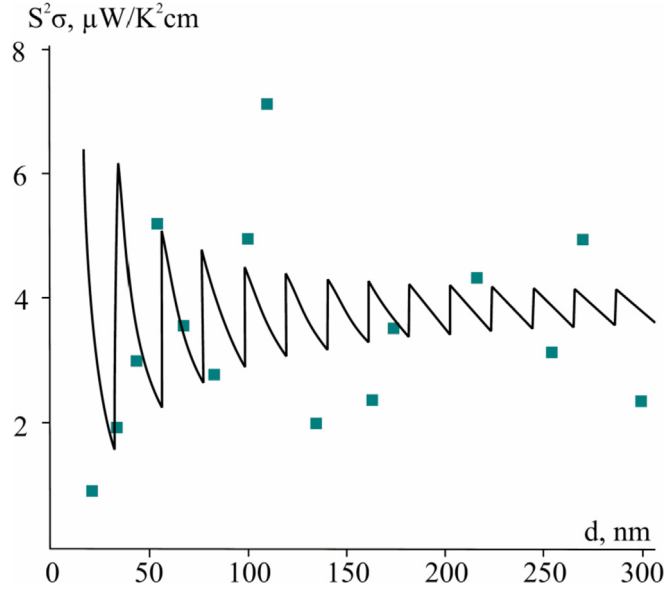


Fig. 15. The thickness dependence of the specific thermoelectric power ($S^2\sigma$) for $\text{Pb}_{14}\text{Sn}_4\text{Ag}_2\text{Te}_{20}$ films deposited on (0001) mica-muscovite substrate in the case of degenerate electron gas. Points are the experiment, line is a calculation.

dependences $S(d)$ and $S^2\sigma(d)$ coincide. However, the minimum of conductivity (σ) corresponds to the maximum of the Seebeck coefficient (S).

The model of the potential well with a flat bottom and infinitely high walls was used to describe of the experimental data for the Seebeck coefficient (S) and the thermoelectric power ($S^2\sigma$). We should consider the degenerate electron gas. We note that in the case of scattering by acoustic phonons, the relaxation time does not depend on energy [33] ($\tau = \tau_0$). In this case, the Seebeck coefficient is defined as [25]:

$$S = \frac{k_B}{e} \left\{ \frac{(\pi^2/3)k_B T [\delta_F - \frac{1}{2} + \sum_{l=1}^{\infty} \frac{\sin(2\pi l \delta_F)}{\pi l}]}{[E_F(\frac{2}{3}\delta_F - \frac{1}{2}) + \frac{\epsilon_1}{2} \sum_{l=1}^{\infty} \frac{\sin(2\pi l \delta_F)}{(\pi l)^3} - \epsilon_1 \sum_{l=1}^{\infty} \frac{\cos(2\pi l \delta_F)}{(\pi l)^2}]} \right\}$$

$$\sigma = \frac{e^2}{\pi d \hbar^2} \frac{1}{2} \tau_0 \left(\left(\frac{m_z}{m_{\perp}} \right)^{1/2} + \left(\frac{m_{\perp}}{m_z} \right)^{1/2} \right) [E_F(\frac{2}{3}\delta_F - \frac{1}{2}) + \frac{\epsilon_1 \delta_F}{2} \sum_{l=1}^{\infty} \frac{\sin(2\pi l \delta_F)}{(\pi l)^3} - \epsilon_1 \sum_{l=1}^{\infty} \frac{\cos(2\pi l \delta_F)}{(\pi l)^2}]$$

where $\delta_F = (\frac{E_F}{\epsilon_1})^{1/2}$, $\epsilon_1 = \frac{\hbar^2}{2m_{\perp}} (\frac{\pi}{d})^2$

The Fermi energy for films with thickness (d) will be determined as follows:

$$E_F(d) = \frac{(n_0 + 1)(2n_0 + 1)}{6} \epsilon_1 + \frac{\pi \hbar^2}{m_{\parallel}} \frac{p}{n_0} d,$$

where n_0 is subband number.

It is known that an increase in the width of quantum well on half-wave Fermi leads to the appearance of new filled sub-band below the Fermi level. At the width of the filling of new band in the density of states we observe a 'jump', which leads to an oscillatory behavior that is shown in the figures.

On the curve $S(d)$, at thickness corresponding to beginning of the filling of new sub-band, a sharp 'jump' occurs on the finite value, just as it does on the curve of the density of states. However, in experimental curves the sharp 'jumps' is not observed, which is due to the blurring of levels by the order of magnitude \hbar/τ . It can be seen from the figures that for small thickness films (~ 50 nm) the amplitude of oscillations is large. The amplitude gradually decreases at the increases of thickness, and at certain thickness it should be close to zero. That is, we get a monotonous change in transport coefficients. In this case, quantization

of the energy spectrum is eliminated and classical regularities will be performed.

It is shown on thickness dependence of thermoelectric figure of merit that the exist of quantum oscillations with a period of (40–50) nm and it reaches values of $S^2\sigma$ to $6 \mu\text{W}/\text{K}^2\text{cm}$ at room temperature (Fig. 15). We take into account that the thermal conductivity of thin film is determined mainly by its substrate, since the volume of the film is small enough. Therefore, we can approximately estimate the value of ZT. The thermal conductivity of mica-muscovite is $\kappa = 2.4 \cdot 10^{-3} \text{ W}/(\text{cm}\cdot\text{K})$ [47]. This result is fully consistent with the above mentioned in this paper for considering thermal diffusivity. Then, the thermoelectric figure of merit $ZT = 0.75$ at $T = 300$ K, and ZT is about 1.5 at 400 K.

These results are much higher than the previous ones. Therefore, taking into account the quantum-size effects it is possible to obtain material with considerably better properties. Furthermore, these results are significantly exceeds such values for thick films or for bulk materials at same temperature.

4. Conclusions

For the first time – the thin films on the basis of new thermoelectric materials – LATT, such as $\text{Pb}_{14}\text{Sn}_4\text{Ag}_2\text{Te}_{20}$, $\text{Pb}_{16}\text{Sn}_2\text{Ag}_2\text{Te}_{20}$ and $\text{Pb}_{18}\text{Ag}_2\text{Te}_{20}$ compounds deposited on mica-muscovite substrates were investigated. All these thin films were characterized by the presence of homogeneously distributed surface nanoscale objects of the pyramidal form.

The temperature and thickness dependences of thermoelectric properties of LATT materials were researched. It is established that the dominant carrier scattering mechanism at temperature range (450–800) K is scattering on acoustic phonons.

For the first time the quantum-size oscillations of thermoelectric parameters have been taken into account, which made it possible to determine the conditions for obtaining their maximum values. It was shown that the $\text{Pb}_{14}\text{Sn}_4\text{Ag}_2\text{Te}_{20}$ films have the highest thermoelectric figure of merit in comparison with the other researched compositions $ZT \sim (1.2–1.5)$ at 400 K. These values are much higher in comparison with the bulk materials based on these compounds.

Funding

Publications are based on the research provided by the grant support of the State Fund For Fundamental Research of Ukraine (project No F73/38–2017).

Authors' contributions

LN performed and determined the problem, and defined the methods and subjects of the investigation as well as made an AFM-images analysis, wrote the manuscript.

MR conducted the theoretical investigate of the quantum-size effects in thin films.

EI developed the theory of the behavior of thermal diffusivity, took part on the defined the methods and subjects of the investigation, interpretation of results.

OK conducted the research of temperature and thickness dependences of the thermoelectric parameters of nanoscale thin films and took a part in the discussion of the experimental results.

IH conducted the experiments, synthesis of multicomponent semiconductor materials, interpreted the results.

IK conducted the experimental research on thermal diffusivity, interpretation of results.

YY conducted the experimental part in thin film technology development and deposition of investigated nanoscale thin films.

AH conducted the experimental investigation of phase composition and structure, interpretation of results.

All authors have read and approved the final version of the

manuscript.

Authors' information

LN is PhD in physical and mathematical sciences, Professor, Vasyl Stefanyk Precarpathian National University, Ivano-Frankivsk, Ukraine.

MR is a doctor of physical and mathematical sciences, Professor, Vasyl Stefanyk Precarpathian National University, Ivano-Frankivsk, Ukraine.

EI is a doctor of physical and mathematical sciences, Professor, B.I. Stepanov Institute of Physics NAS of Belarus, Minsk, Belarus.

OK is PhD student at the Physics and Chemistry of Solid State Department, Vasyl Stefanyk Precarpathian National University, Ivano-Frankivsk, Ukraine.

IH is Ph.D in physical and mathematical sciences, post-doc, Vasyl Stefanyk Precarpathian National University, Ivano-Frankivsk, Ukraine.

IK is PhD of physical and mathematical sciences, researcher, B.I. Stepanov Institute of Physics NAS of Belarus, Minsk, Belarus.

YY is Ph.D in physical and mathematical sciences, Vasyl Stefanyk Precarpathian National University, Ivano-Frankivsk, Ukraine.

AH is Ph.D in physical and mathematical sciences, Vasyl Stefanyk Precarpathian National University, Ivano-Frankivsk, Ukraine.

Journal *Physica E: Low-dimensional Systems and Nanostructures* is the famous scientific journal on the topic of investigation of the physical properties of the low-dimensional systems. In this paper it is shown the possibility to receive the high-effectively thermoelectric material in form of two-dimension nanoscale thin films. The best results are explained by methods of quantum-size effects that are manifested precisely only in nanoscale systems.

Therefore, the publishing in *Physica E: Low-dimensional Systems and Nanostructures Journal* is the opportunity to showcase new results for the scientific community, whose representatives the best world-class specialists. In this way, scientific results will become more accessible.

Competing interests

The author declares that he has no competing interests.

Acknowledgements

This work was performed under the Laboratory of Physical and Technical Department, Vasyl Stefanyk Precarpathian National University in Ivano-Frankivsk, Ukraine and Laboratory of optical holography B.I Stepanov Institute of Physics in Minsk, Belarus.

References

- G.J. Snyder, E.S. Toberer, Complex thermoelectric materials, *Nat. Mater.* 7 (2008) 2–105.
- E. Couderc, Thermoelectrics: invisible harvest, *Nat. Energy* 2 (2017) 17137, <https://doi.org/10.1038/nenergy.2017.137>.
- L.D. Zhao, V.P. Dravid, M.G. Kanatzidis, The panoscopic approach to high performance thermoelectrics, *Energy Environ. Sci.* 7 (2014) 251–268, <https://doi.org/10.1039/C3EE43099E>.
- D.M. Rowe, *Thermoelectrics Handbook: Macro to Nano*, CRC/Taylor & Francis, Boca Raton, 2006.
- Y. Pei, Z.M. Gibbs, B. Balke, W.G. Zeier, G.J. Snyder, Optimum Carrier concentration in n-type PbTe thermoelectrics, *Adv. Energy Mater.* 4 (2014) 1400486.
- Z. Chen, Z. Jian, W. Li, Y. Chang, B. Ge, R. Hanus, J. Yang, Y. Chen, M. Huang, G.J. Snyder, Y. Pei, Lattice dislocations enhancing thermoelectric PbTe in addition to band convergence, *Adv. Mater.* 29 (2017) 1606768.
- Y. Pei, L. Zheng, W. Li, S. Lin, Z. Chen, Y. Wang, X. Xu, H. Yu, Y. Chen, B. Ge, Interstitial point defect scattering contributing to high thermoelectric performance in SnTe, *Adv. Electronic Mater.* 2 (2016) 1600019.
- W. Li, L. Zheng, B. Ge, S. Lin, X. Zhang, Z. Chen, Y. Pei, Promoting SnTe as an eco-friendly solution for p-PbTe thermoelectric via band convergence and interstitial defects, *Adv. Mater.* 29 (2017), <https://doi.org/10.1002/adma.201605887>.
- E.I. Rogacheva, O.N. Nashchekina, T.V. Tavrina, M. Us, Mildred S. Dresselhaus, Steve B. Cronin, Oded Rabin, Quantum size effects in IV–VI quantum wells, *Phys. E Low-dimens. Syst. Nanostruct.* 17 (2003) 313–315.
- D.M. Freik, S.I. Mudryi, I.V. Gorichok, R.O. Dzumedzey, O.S. Krynytskiy, T.S. Lyuba, Charge Carrier scattering mechanisms in thermoelectric PbTe: Sb, *Ukrainian J. Phys.* 59 (2014) 706–711.
- K.F. Hsu, S. Loo, F. Guo, W. Chen, J.S. Dyck, C. Uher, M.G. Kanatzidis, Cubic $\text{AgPb}_m\text{SbTe}_{2+m}$: bulk thermoelectric materials with high figure of merit, *Science* 303 (2004) 818–821.
- I. Horichok, R. Ahiska, D. Freik, L. Nykyruy, S. Mudry, O. Matkivskiy, T. Semko, Phase content and thermoelectric properties of optimized thermoelectric structures based on the Ag-Pb-Sb-Te system, *J. Electron. Mater.* 45 (2016) 1576–1583.
- H.S. Dow, M.W. Oh, S.D. Park, B.S. Kim, B.K. Min, H.W. Lee, D.M. Wee, Thermoelectric properties of $\text{AgPb}_m\text{SbTe}_{m+2}$ ($12 \leq m \leq 26$) at elevated temperature, *J. Appl. Phys.* (2009) 113703, <https://doi.org/10.1063/1.3138803>.
- J.R. Sootsman, D.Y. Chung, M.G. Kanatzidis, New and old concepts in thermoelectric materials, *Angew. Chem. Int. Ed.* 48 (2009), <https://doi.org/10.1002/anie.200900598>.
- Z. Tian, J. Garg, K. Esfarjani, T. Shiga, J. Shiomi, G. Chen, Phonon conduction in PbSe, PbTe, and $\text{PbTe}_{1-x}\text{Se}_x$ from first-principles calculations, *Phys. Rev. B* 85 (2012) 184303, <https://doi.org/10.1103/PhysRevB.85.184303>.
- W. Heng, Y. Pei, A.D. LaLonde, G. Jeffery Snyder, Material design considerations based on thermoelectric quality factor, in: K. Kunihiro, T. Mori (Eds.), *Thermoelectric Nanomaterials*, Springer, Berlin, Heidelberg, 2015, pp. 3–32.
- M. Bala, A. Bhogra, S.A. Khan, T.S. Tripathi, S.K. Tripathi, D.K. Avasthi, K. Asokan, Enhancement of thermoelectric power of PbTe thin films by Ag ion implantation, *J. Appl. Phys.* 121 (2017) 215301.
- H. Wang, J.F. Li, T. Kita, Thermoelectric enhancement at low temperature in nonstoichiometric lead-telluride compounds, *J. Phys. D: Appl. Phys.* 40 (2007) 6839.
- Z. Dashevsky, R. Kreizman, M.P. Dariel, Physical properties and inversion of conductivity type in nanocrystalline PbTe films, *J. Appl. Phys.* 98 (2005) 094309, <https://doi.org/10.1063/1.2126785>.
- M.O. Haluschak, S.I. Mudryi, M.A. Lopyanko, S.V. Optasyuk, T.O. Semko, L.I. Nikiryu, I.V. Horichok, Phase composition and thermoelectric properties of materials in Pb-Ag-Te system, *J. Thermoelectricity* 3 (2016) 34–39.
- D.M. Zayachuk, P.M. Starik, V.A. Shenderovskii, The effect of nonstoichiometric tellurium on the properties of lead and tin tellurides, *Phys. Status Solidi (a)* 107 (1998) 95–99.
- J.P. Heremans, M.S. Dresselhaus, L.E. Bell, D.T. Morelli, When thermoelectrics reached the nanoscale, *Nat. Nanotechnol.* 8 (2013) 471, <https://doi.org/10.1038/nnano.2013.129>.
- L.D. Hicks, M.S. Dresselhaus, Effect of quantum-well structures on the thermoelectric figure of merit, *Phys. Rev. B* 47 (1993) 12727.
- M.P. Singh, C.M. Bhandari, Non-monotonic thermoelectric behavior of lead telluride in quantum-well-like structures, *Solid State Commun.* 133 (2005) 29–34.
- M.A. Ruvinskii, O.B. Kostyuk, B.S. Dzundza, The influence of the size effects on the thermoelectric properties of PbTe thin films, *J. Nano Electronic Phys.* 8 (2016) 02051, [https://doi.org/10.21272/jnep.8\(2\).02051](https://doi.org/10.21272/jnep.8(2).02051).
- I.V. Horichok, M.O. Galuschak, O.M. Matkivskiy, I.P. Yaremij, R.Y. Yavorskyj, V.S. Blahodyr, O.I. Varunkiv, T.O. Parashchuk, Thermoelectric properties of nanostructured materials based on lead telluride, *J. Nano- Electronic Phys.* 9 (2017) 05022.
- R. Venkatasubramanian, E. Silvola, T. Colpitts, B. O'quinn, Thin-film thermoelectric devices with high room-temperature figures of merit, *Nature* 413 (2001) 597.
- A. Boyer, E. Cisse, Properties of thin film thermoelectric materials: application to sensors using the Seebeck effect, *Mater. Sci. Eng., B* 13 (1992) 103–111, [https://doi.org/10.1016/0921-5107\(92\)90149-4](https://doi.org/10.1016/0921-5107(92)90149-4).
- J. Mao, Z. Liu, Z. Ren, Size effect in thermoelectric materials, *npj. Quant. Mater.* 1 (2016) 16028.
- E.I. Rogacheva, O.N. Nashchekina, S.N. Grigorov, M.A. Us, M.S. Dresselhaus, S.B. Cronin, Oscillatory behaviour of the transport properties in PbTe quantum wells, *Nanotechnology* 14 (2002) 53.
- B.S. Dzundza, O.B. Kostyuk, V.I. Makovyshyn, The thickness dependence of thermoelectric parameters of thin films based on compounds LAST, *Phys. Chem. Solid State* 17 (2016) 368–371, <https://doi.org/10.15330/pcss.17.3.368-371>.
- X. Chen, D. Parker, D.J. Singh, Importance of non-parabolic band effects in the thermoelectric properties of semiconductors, *Sci. Rep.* 3 (2013) 3168, <https://doi.org/10.1038/srep03168>.
- H. Yokoi, S. Takeyama, O. Portugall, N. Miura, G. Bauer, Anomalous temperature dependence of the effective mass in PbTe and PbSe, *Phys. B Condens. Matter* 184 (1993) 173–177, [https://doi.org/10.1016/0921-4526\(93\)90344-6](https://doi.org/10.1016/0921-4526(93)90344-6).
- S. Venkatapathi, Temperature Effects on the Electronic Properties of Lead Telluride (PbTe) and the Influence of Nano-size Precipitates on the Performance of Thermoelectric Materials (SrTe Precipitates in PbTe Bulk Material), *Diss. Virginia Tech, Virginia*, 2013.
- D.M. Zayachuk, V.I. Mikityuk, V.M. Frasunyak, V.V. Shlemkevych, High temperature transformation in the defects and impurities system of PbTe:Eu crystals, *J. Cryst. Growth* 311 (2009) 4670–4674.
- X. Zhang, Y. Pei, Manipulation of charge transport in thermoelectrics, *npj Quant. Mater.* 2 (2017) 68, <https://doi.org/10.1038/s41535-017-0071-2>.
- Y. Pei, H. Wang, G.J. Snyder, Band engineering of thermoelectric materials, *Adv. Mater.* 24 (2012) 6125–6135.
- Z.M. Gibbs, H. Kim, H. Wang, R.L. White, F. Drymiotis, M. Kaviani, Jeffrey G. Snyder, Temperature dependent band gap in PbX ($X = \text{S, Se, Te}$), *Appl. Phys. Lett.* 103 (2013) 262109.
- M.A. Ruvinskii, O.B. Kostyuk, B.S. Dzundza, I.P. Yaremij, M.L. Mokhnatskiy, Y.S. Yavorskyj, Kinetic phenomena and thermoelectric properties of polycrystalline thin films based on PbSnAgTe compounds, *J. Nano Electronic Phys.* 9 (2017) 05004, [https://doi.org/10.21272/jnep.9\(5\).05004](https://doi.org/10.21272/jnep.9(5).05004).

- [40] I.V. Horichok, L.I. Nykyruy, T.O. Parashchuk, S.D. Bardashevskaya, M.P. Pylyponuk, Thermodynamics of defect subsystem in zinc telluride crystals, *Mod. Phys. Lett. B* 30 (2016) 1650172, , <https://doi.org/10.1142/S0217984916501724> 30:16.
- [41] A.N. Shimko, G.E. Malashkevich, D.M. Freik, L.I. Nykyruy, V.G. Lytovchenko, Effect of thermal treatment of PbTe films on their IR spectra and surface structure, *J. Appl. Spectrosc.* 80 (2014) 950–953.
- [42] D.M. Freik, S.I. Mudryi, I.V. Gorichok, V.V. Prokopiv, O.M. Matkivsky, I.O. Arsenjuk, O.S. Krynytsky, V.M. Bojchyk, Thermoelectric properties of bismuth-doped tin telluride SnTe:Bi, *Ukrainian J. Phys.* 61 (2016) 155–159.
- [43] E.V. Ivakin, I.G. Kisialiou, O.L. Antipov, Laser ceramics Tm:Lu₂O₃. Thermal, thermo-optical, and spectroscopic properties, *Opt. Mater.* 35 (2013) 499–503.
- [44] J.A. Johnson, A.A. Maznev, K.A. Nelson, M.T. Bulsara, E.A. Fitzgerald, T.C. Harman, S. Calawa, C.J. Vineis, G. Turner, Phase-controlled, heterodyne laser-induced transient grating measurements of thermal transport properties in opaque material, *J. Appl. Phys.* 111 (2012) 023503, , <https://doi.org/10.1063/1.2675467>.
- [45] K. Kishimoto, M. Tsukamoto, T. Koyanagi, Temperature dependence of the Seebeck coefficient and the potential barrier scattering of n-type PbTe films prepared on heated glass substrates by rf sputtering, *J. Appl. Phys.* 92 (2002) 5331–5339.
- [46] A.J. Schmidt, X. Chen, G. Chen, Pulse accumulation, radial heat conduction, and anisotropic thermal conductivity in pump-probe transient thermoreflectance, *Rev. Sci. Instrum.* 79 (2008) 114902.
- [47] M.F. Brigatti, S. Guggenheim, Mica crystal chemistry and the influence of pressure, temperature, and solid solution on atomistic models, *Rev. Mineral. Geochem.* 46 (2002) 1–97.